15th Triennial World Congress, Barcelona, Spain

POWER CONTROL OF A BRUSHLESS PERMANENT MAGNET ELECTRIC MACHINE FOR EXERCISE BIKES

Tung-Chang Tsai and Mi-Ching Tsai

Department of Mechanical Engineering, National Cheng Kung University, Tainan 701, Taiwan

Abstract: This paper presents a power control structure for a brushless permanent magnet electric machine, where both generating and motoring operation modes using the same power stage coexist using a digital control scheme. In the generating mode, desired dynamic output such as constant power and constant torque can be achieved for use in an exercise bicycle, where the input power generated by pedaling is transferred into the battery in the form of electrical energy to provide braking resistance, known as the regenerative braking. The user controls the resistance via a closed-loop torque controller to the desired exercise, also the study uses three position Hall sensors instead of an expensive encoder, to perform the commutation and speed estimation. Both the theoretical derivation and experimental verification for the proposed control scheme are presented in this paper, which is implemented using a TI TMS320F240 digital signal processor. *Copyright © 2002 IFAC*

Keywords: Brushless permanent magnet electric machine; exercise bike; regenerating braking; DSP.

1. INTRODUCTION

Due to a higher standard of living and more attention being paid to health, exercise bikes as shown in Fig. 1 have become increasingly popular indoor exercise equipment. One of the main components used in moderns exercise bikes is an electric machine (EM). The EM rotates as the user pedals the bike, which generates electric power and provides the user with a resistant force that can be adjusted to satisfy the user's exercising demand. The conventional approach to create and adjust resistance is to use either friction braking or dynamic braking techniques, where kinetic energy is completely dissipated in the form of heat (Ong, 1998; Bexerra, et al., 1992). These methods basically satisfy the exercise bike function, however from an energy recycling point of view, this rather wasteful and can be improved to make use of the energy from the user for other purposes. Therefore, in this paper an approach named regenerative braking is presented and applied to exercise bikes. This not only controls and regulates the resistance, but also recycles the dissipated kinetic energy into a battery in the form of electric energy. The energy can be used in the motoring mode of the EM to actively drive the user into movement for medical rehabilitation, thus combining exercising and rehabilitation into one bike (Cybex, 1992).

This paper presents a generating/motoring mode coexisting structure (G/MMCS) as shown in Fig. 2 (detailed later), which utilizes multi-quadrant operation. Therefore, the above resistant control technique and the G/MMCS can increase efficiency and provide a variety of functions for exercise bikes, which usually only operate in one mode.

In the EM's torque-speed plane, there are four steady-state modes of operation as shown in Fig. 3 (Becerra, et al., 1992). Quadrants I and III are forward and reverse motoring respectively. In quadrants II and IV, which are forward and reverse braking respectively, the torque and the speed have opposite polarities such that the torque provides a resistive force and the EM generates power (Bexerra, et al., 1991; Bexerra, et al., 1992; Jahns, et al., 1991). Theoretically, the generator and the motor can properly work using the same power hardware. Torque control of the brushless permanent magnet electric machine (BLPMEM) in the motoring mode with 120° trapezoidal excitation has been reported

in a previous publication (Chu. et al., 2001). In contrast, this paper is devoted to the study of the generating mode in a BLPMEM and implements a regenerative braking technique using a commercially available digital signal processor (DSP) to achieve the resistance control for the exercise bike.

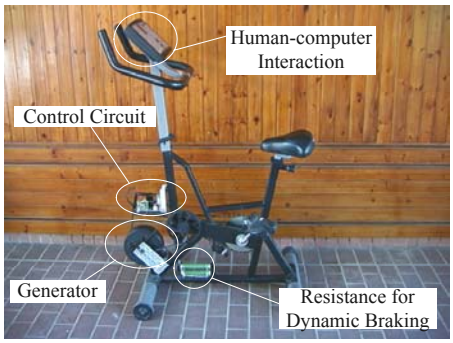

Fig. 1. A commercially available exercise bike

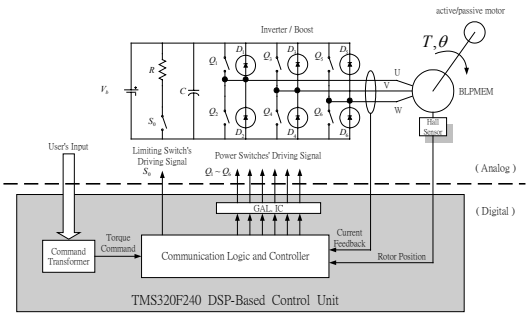

Fig. 2. Generating/motoring mode coexisting structure

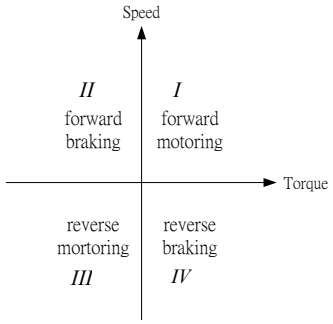

Fig. 3. Four-quadrant operation

The BLPMEM can be treated as a DC machine in the following way:

The torque, which is function of the driving current, can be controlled by regulating the phase current (Rizzoni, 2000). Therefore, the desired torque response, i.e., the required resistance, can be achieved by controlling the phase current. Enabling a switching pattern of the power stage according to the rotor position sensor will produce a current in the target winding (as seen in Fig. 2). When the current rises beyond the command value, a set of switches is turned off and then the energy stored in the winding circulates through the diodes, the repetition of this operation regulates the phase current. Current regulation controls the rate of power flow from the supply to the load during the motoring operation as well as that from the load to the supply in the generating mode. Moreover, commutation of the BLPMEM is performed electronically instead of mechanically, and hence no mechanical commutator is needed and the sparking problem is also avoided.

This paper is outlined as follows. Section 2 introduces the overall system architecture, followed by Section 3, which discusses the principle of regenerative braking. The power control algorithm using a TI TMS320F240 DSP is then described in Section 4. In Section 5, experimental results are presented to verify the effectiveness of the proposed design and finally a brief conclusion is given in Section 6.

2. SYSTEM ARCHITECTURE

A DSP-based digital power control scheme for the G/MMCS is shown in Fig. 2 where the system consists of a BLPMEM, a power stage, a resistance-switch set, a battery and a control unit. The BLPMEM used here has a trapezoidal back EMF, generally known as the brushless DC machine with current flowing in only two phases in the motoring mode at any given time instant (Rizzoni, 2000). For a trapezoidal back EMF with a 120° flat top and pulsewidth modulated (PWM) rectangular current excitation. The torque produced is rectangular with an interval of 120° and its polarity depends on the operational mode. Ideally, the total torque is constant (ripple free). Figure 4 shows an ideal sketch of the back EMF, the current for each phase and the total torque produced in the motoring operation of the BLPMEM.

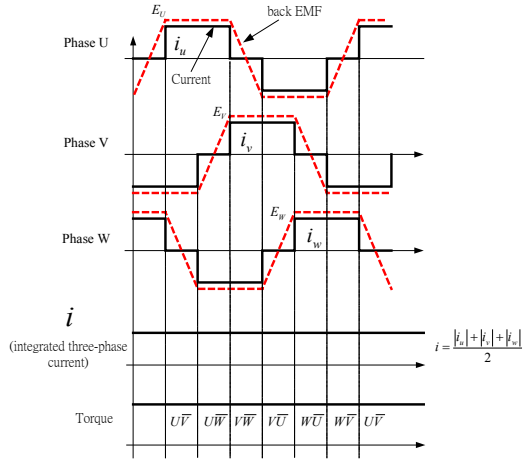

Fig. 4. Waveforms of a BLPMEM with 120-degree drive

The power stage is composed of six bilateral PWM IGBT power switches (Q1~Q6) and six diodes (D1~D6), which is a voltage source boost/inverter (see Fig. 3) and is used to drive the three-phase generator/motor. It helps the system achieve the dynamic demand by controlling the winding current. The power from the battery is dissipated on the motor to reach the aimed torque in the motoring mode.

Contrarily, the power stored in the three-phase winding is delivered to the charged battery to achieve resistance control for exercise bikes.

Finally, it is useful to introduce a resistance in parallel with the power stage, as seen in Fig 2, in order to protect the entire hardware from dangerous situations, caused by increasing the voltage of the battery while the system is in the process of charging. When the voltage of the battery rises above the rated value, a limit switch (S_0) is turned on so the output current of the generator flows through the resistance instead of the battery, which is often known as dynamic braking (Ong, 1998).

3. OPERATING PRINCIPLE OF REGENERATIVE BRAKING

The BLPMEM has three trapezoidal phase-back EMFs of equal amplitude and a frequency displaced in phase by 120°. When operating in the generating mode, the switching topology is based on the maximum line-to-line back EMF for more energy charging. According to the above-mentioned principle, an appropriate switching pattern for regenerative braking in one electric period is shown in Fig. 5 (Kim, et al., 1998). A boost is needed in practice to raise the back EMF, this done with one type of the dc-dc switching converter, and then the EM generates a current whose direction is opposite to that in the motoring mode supplying power to the load.

Taking the duration from 60° to 120° shown in Fig. 5 as an example, phases U and V should be excited. In that duration, switch Q2 is pulsewidth modulated and the other switches are off, as indicated in Fig. 6(a), where it can be seen that when Q2 is turned on, the current gradually increases and flows through switch Q2 and diode D4. When Q2 is turned off, the energy stored in phase U and V is diverted back to the battery through diode D1 and D4 as shown in Fig. 6(b). Switching patterns for other durations can be found using the same rules.

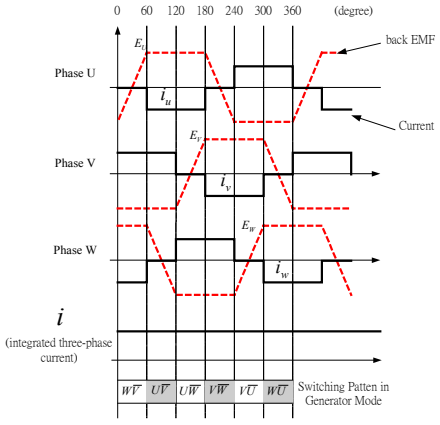

Fig. 5. Operation of regenerative braking of a BLPMEM

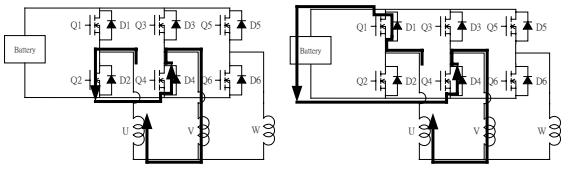

Fig. 6. Circuits during regeneration for phases U and V: (a) Q2 is turned on; (b) Q2 is turned off

4. POWER CONTROL ALGORITHM

In Fig. 7, a closed-loop torque control scheme, which consists of three main parts: the speed estimator, the torque command transformer and the torque controller, is proposed to achieve the dynamic demand of constant power/torque resistance, where the control algorithm is implemented in real-time using a DSP in an experimental setup. The user's command is first sent to the torque command generator, which computes the corresponding torque command based on the feedback speed. The torque command is then handed over to the torque controller, where the driving signals of the power stage are computed to produce the regulated phase current, the desired torque response can then be reached. The speed is calculated with an estimator using the signals from Hall position sensor, which are also the basis of commutation in the BLPMEM.

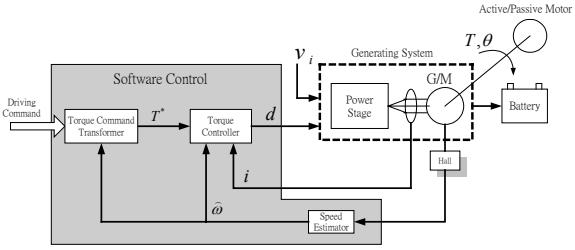

Fig. 7. Closed loop control structure

4.1 Speed Estimation

Practically, speed information is often acquired via signals from the rotor position sensor in a servo control system. For the dynamic application in the present study, it is appropriate to estimate the speed by measuring the duration between the two successive position pulses generated by the Hall sensors, which are selected for their low cost and precision at variable speeds in the proposed application. Speed can therefore be calculated using the following equation

$$\omega = \frac{1/P}{\frac{1}{f_c} \times n_c} \times 60 = \frac{60 f_c}{P n_c} \quad \text{(rpm)} \qquad (1)$$

where P is the number of pulses per revolution, n_c is the number of timed pulses between the two successive position pulses, where f_c is the frequency of the timer. In the experiment, the capture unit on the DSP card can detect the rising/falling edges of the

3-bit Hall sensor signals to obtain the position pulses as shown in Fig. 8.

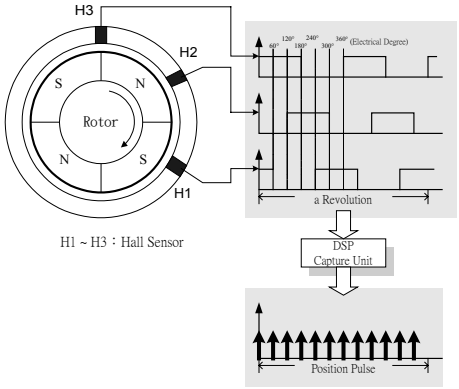

Fig. 8. Speed calculation of a BLPMEM

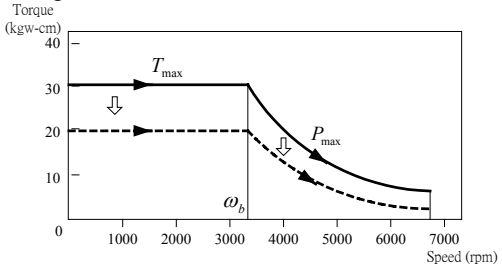

Fig. 9. Torque command transformer

4.2 Torque Command Transformation

Different personal fitness goals can be determined by oneself and range from simply improving one's ability to perform everyday tasks to feeling more energized and being able to ride a hundred miles on a bicycle or bench pressing one's body weight. Clinically, many health advisors administer exercise tests over a velocity spectrum in which slow, intermediate and high-speed repetitions are performed. The slow speed test provides a good indication of one's ability to withstand compressive forces (which causes one to produce higher peak torque) and the best information for peak torque/body weight ratio. While the importance of intermediate and high-speed exercising tests lies in a more accurate measurement of the energy produced and performing endurance exercise (which contrarily causes one to produce lower peak torque but higher power). Therefore, a well-scheduled torque curve of the exercise bike is crucial and can make the user strive for improvement, enjoyment and physical benefit (Cybex, 1992).

Having decided the BLPMEM work area, in this paper the low-speed area is designed to operate in a constant torque resistance, in which the bike's user prepares for a more intensive workout from a slow and easy warm-up. The intermediate and high-speed areas are designed to operate in a constant power resistance, in which the torque curve allows the user to take endurance exercise for better overall physical fitness. Also, the user's muscles and cardiovascular system can be trained to operate more powerfully and efficiently. Thus properly structured exercise sessions can be accomplished with the curve arranged in Fig. 9, where the base speed determines the boundary between the constant torque and the constant power regions. This EM is in fact controlled at a constant torque resistance when the EM speed ω is less than the base speed ω_b, and is controlled at constant power resistance when the EM speed is greater than the base speed.

The rule for the torque command generation from user's input is explained below. First, the maximum torque $T_{\max}$, the base speed ω_b and the maximum power $P_{\max}$ are required and their relation is given by

$$P_{\max} = T_{\max} \times \omega_b \quad (2)$$

The torque command can therefore be expressed by the following equations, where the transition between the above two dynamic characteristics is according to the base speed

$$T_{cmd} = Command \times T_{\max} \quad \text{as} \quad \omega < \omega_b \quad (3)$$

$$T_{cmd} = \frac{Command \times P_{\max}}{\omega} \quad \text{as} \quad \omega \geq \omega_b \quad (4)$$

$$Command = 0 \sim 1 \quad (5)$$

The measured results from the two software controlled exercise sessions are discussed in Section 5, where two different command patterns are investigated.

4.3 Torque Constant in Generating Mode

As shown in Fig. 10, the desired torque command should be transformed into the current command by a torque constant k_{tg}, in the generating mode, and this current command is then regulated in the current loop by controlling the duty cycle of the power stage. Since the magnitude of the back EMF in the BLPMEM is not an ideal for the level of DC (see Fig. 11), the equivalent value of k_{tg} is in fact not a constant and depends on the operating speed. For accurately transforming the desired torque commands into current commands, a method by adding a modification factor k (ranging between 0 and 1) is proposed to solve this problem, as described in the following.

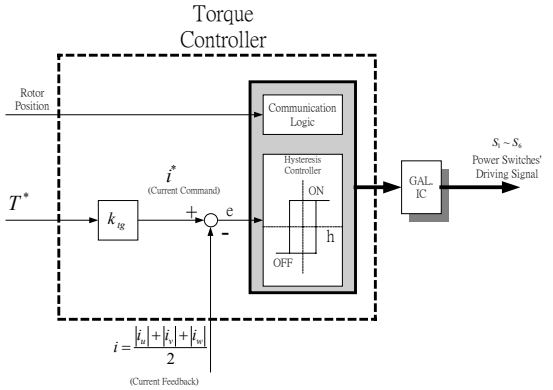

Fig. 10. Torque Controller

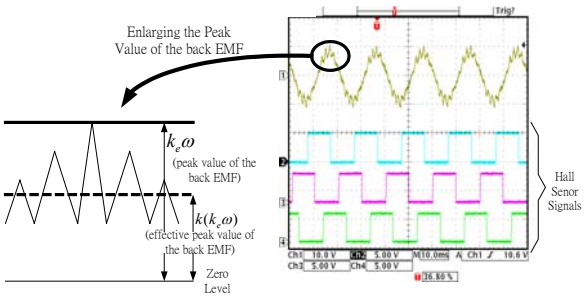

Fig. 11. Correction of torque constant in the generating mode

By neglecting power losses in the whole process, the input mechanical power equals the output electrical power. Therefore,

$$P = T\omega = EI = (k_e\omega)I \tag{6}$$

where T is the machine torque, ω is the EM's speed, E is the EM's back EMF, I is the phase current and k_e is the back EMF constant. By introducing a modification factor k, Eqn. (6) can be rewritten as

$$T\omega = (kk_e\omega)I \tag{7}$$

so that

$$T = (kk_e)I = k_{tg}I \tag{8}$$

$$k_{tg} = kk_e \tag{9}$$

Obviously, if k=1, then $k_{tg} = k_e$, i.e., k_{tg} is equal to the torque constant, k_t, in the motoring mode. In the qualitative analysis performed by observation, the back EMF of the DC BLPMEM is more like a trapezoidal waveform at the intermediate and high-speed regions, so that the modified factor k is closer to 1. Contrarily, a smaller k is needed at the low-speed region.

4.4 Commutation Logic and Current Control Unit

In this proposed G/MMCS, the commutation logic and current control unit is the core of the control system and performs commutation and current regulation (see Fig. 10). As previously mentioned, the commutation of the BLPMEM is based on the feedback signals of the Hall sensors. Since the whole generating system, which is inherently a pulsewidth modulated power electronic structure is complicated by its switching behavior it cannot be modeled accurately. A hysteresis control strategy is adopted here in the current loop to overcome inherent uncertainties and nonlinearities (Sun, et al., 1999; Mascarenhas, 1992). Finally, the driving signals are delivered through the GAL (Gate Array Logic) IC (also see Fig. 10), which is set up to avoid the shoot-through fault between an upper and lower power devices placed in series on one power converter leg to the power stage.

5. EXPERIMENTAL RESULTS

In the experimental setup, the G/MMCS is assembled with the dynamometer and other measuring equipment to form an experimental platform. The implementation of the system shown in Fig. 2 consists of the power stage described in the previous section and the TMS320F240 control unit. In the DSP-based control unit, the TMS320F240 is equipped with three independent timers, 28 individually programmable/multiplexed I/O pins, 16 bits data bus, 544 words data/program dual-access RAM, dual 10-bit A/D converter, 4-channel 12-bit D/A converter and the RS232 communication port. All the information sensed into the DSP chip is assigned to several tasks. Circuit performance is assessed on a number of parameters, the current control loop takes 50 μs where the PWM frequency for the power switch is set to 20 KHz.

A prime mover is used to rotate the BLPMEM at a fixed speed for obtaining the steady state regeneration. The experiments are undertaken with the system parameters listed in Table 1 for verifying the validity of the proposed design methods. The results are given in the generating mode over the speed range from 0 to 5400 rpm. Figures 12 and 13 show the oscillograms for the regenerative braking scheme with current commands at 35 and 50 A respectively. The lower curves of Figs. 12(a) and 13(a) show a typical EM current in phase U and the upper parts represent the gate signal for the lower switch (Q2) of phase U. Figures 12(b) and 13(b) show the integrated three-phase current ($i = \frac{|i_u| + |i_v| + |i_w|}{2}$) of the EM with current commands also at 35 and 50 A respectively.

As mentioned before, ideally, the rectangular current excitation of the BLPMEM should have a constant torque. However, from Figs. 12 and 13, there is only as quasi-rectangular current waveforms to be obtained in practice. The main reasons are as follows:

(1) The winding inductance L of the BLPMEM is not a constant, but a quasi-sinusoidal distribution that depends on the rotor position.
(2) The magnitude of the BLPMEM back EMF is not an ideal DC level.
(3) The transient response of voltage of the battery is neglected.

Figure 14 shows the measured result obtained from the proposed closed loop torque control, where the maximum torque $T_{\max}$=30 (kgw-cm), the base speed $\omega_b = 3300$ (rpm) and the maximum power $P_{\max}$=964.68 (W). Note that the specified dynamic characteristic of the BLPMEM in the generating mode is often divided into two parts by the base speed: the constant torque and the constant power region. In this experiment, a modification factor k is chosen to be 1 while the EM speed is beyond 4500 rpm and 0.8 while the EM speed is lower than that

speed respectively. The experimental results have confirmed the effectiveness of the proposed closed-loop torque control scheme in which the desired torque-speed characteristic can be achieved in the generating mode.

TABLE 1. BLPMEM parameters

Term	Description
Rated voltage	48 V
Rated power	0.58 kW
Rotor poles	4
k_e	5.45×10^{-3} V/rpm
Winding inductance	117.25 μ H

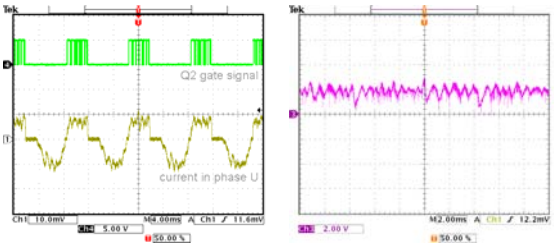

(a) (b)

Fig. 12. Dynamic response of current control (I^* =35 A, ω =3000 rpm): (a) Phase U current (50A/div); (b) Current response composed of three phases (40A/div)

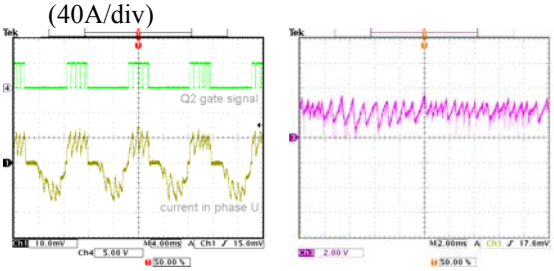

(a) (b)

Fig. 13. Dynamic response of current control (I^* =50 A, ω =3000 rpm): (a) Phase U current (50A/div); (b) Current response composed of three phases (40A/div)

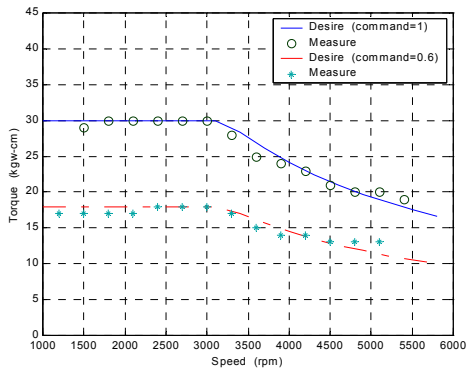

Fig. 14. Measured results of torque control from software controller

6. CONCLUSIONS

In this study a generating/motoring mode coexisting structure possessing multi-quadrant operational ability and a novel resistance control technique using regenerative braking for exercise bikes have been introduced. Also, a BLPMEM, a power stage, a resistance-switch set, a battery and a control unit based on DSP are employed to construct the experimental system. Via a proposed digital control scheme, the brushless permanent-magnet electric machine in the generating mode can output the requiring dynamic performance such that a constant power and constant torque resistance achieve the user's exercise requirements. The satisfactory dynamic responses have shown the capability and feasibility of the proposed control scheme.

ACKNOWLEDGEMENTS

The author is grateful to the National Science Council of the Republic of China for supporting this research under the grant NSC89-EPA-Z-006-007.

REFERENCES

Becerra, R. C., Ehsani, M. and Jahns T. M. (1991). Four-quadrant sensorless brushless ECM drive. *IEEE Transactions on Power Electronics*, **6**, Issue 1, 118-126.

Becerra, R. C., Ehsani, M. and Jahns T. M. (1992). Four-quadrant brushless ECM drive with integrated current regulation. *IEEE Transactions on Industry Applications*, **28**, Issue 4, 833-841.

Chu, C. L., Tsai M. C., and Chen H. Y. (2001). Torque Control Of Brushless DC Motors Applied To Electric Vehicles. *IEMDC 2001 Conference Proceedings*, 82-87.

Cybex Division of Lumex Inc. (1992). *Cybex 6000 Testing and Rehabilitation System User's Guide,* Revision C.

Jahns T. M., Becerra, R. C. and Ehsani, M. (1991). Integrated current regulation for a brushless ECM drive. *IEEE Transactions on Power Electronics*, **6**, Issue 1, 118-126.

Kim, W. H. Kim, J. S., Raek J. W., Ryoo, H. J. and Rim, G. H. Improving efficiency of flywheel energy storage system with a new system configuration. *PESC 98 Conference Proceedings*, **1**, 24-28.

Mascarenhas E. J. P. (1992). Hysteresis control of a continuous boost regulator. *IEE Colloquium on Static Power Conversion.*

Ong, C. M. (1998). *Dynamic simulation of electric machinery :using Matlab/Simulink*, Prentice Hall PTR.

Rizzoni G. (2000). *Priciples and Applications of Electrical Engineering*, McGraw-Hill.

Sun, C. X., Lehman B. and Ciprian R. (1999). Dynamic modeling and control in average current mode controlled PWM DC/DC converters. *PESC 99 Conference Proceedings,* **2**, 1152-1157.